



## The Sardinia Radio Telescope

G. Grueff<sup>1</sup>, G. Alvitto<sup>2</sup>, R. Ambrosini<sup>1</sup>, P. Bolli<sup>1</sup>, N. D'Amico<sup>2,4</sup>, A. Maccaferri<sup>1</sup>,  
G. Maccaferri<sup>1</sup>, M. Morsiani<sup>1</sup>, L. Mureddu<sup>2</sup>, V. Natale<sup>3</sup>, L. Olmi<sup>3</sup>, A. Orfei<sup>1</sup>,  
C. Pernechele<sup>2</sup>, A. Poma<sup>2</sup>, I. Porceddu<sup>2</sup>, L. Rossi<sup>1</sup>, and G. Zacchioli<sup>1</sup>

<sup>1</sup> INAF, Istituto di Radioastronomia - Sezione di Bologna, Via P. Gobetti, 101, I-40129 Bologna

<sup>2</sup> INAF, Osservatorio Astronomico di Cagliari, Loc. Poggio dei Pini, Strada 54, I-09012 Capoterra (Cagliari)

<sup>3</sup> INAF, Istituto di Radioastronomia - Sezione di Firenze, Largo E. Fermi, 5, I-50125 Firenze

<sup>4</sup> Università degli Studi di Cagliari, Dipartimento di Fisica, SP Monserrato-Sestu, Km 0.700, I-09042 Monserrato (Cagliari)

**Abstract.** We describe the Sardinia Radio Telescope (SRT), a new general purpose, fully steerable antenna of the National Institute for Astrophysics. The radio telescope is under construction near Cagliari (Sardinia). With its large aperture (64m diameter) and its active surface, SRT is capable of operations up to  $\sim 100$ GHz, it will contribute significantly to VLBI networks and will represent a powerful single-dish radio telescope for many science fields. The radio telescope has a Gregorian optical configuration with a supplementary beam-waveguide (BWG), which provides additional focal points. The Gregorian surfaces are shaped to minimize the spill-over and standing wave. After the start of the contract for the radio telescope structural and mechanical fabrication in 2003, in the present year the foundation construction will be completed. The schedule foresees the radio telescope inauguration in late 2006.

**Key words.** Ground-based radio-telescopes, Radioastronomy, active surface

### 1. Introduction

The Sardinia Radio Telescope (SRT) is a challenging scientific project managed by the National Institute for Astrophysics (INAF). The project is funded by the Italian Ministry of Education and Scientific Research and by the Sardinia Regional Government.

SRT is a fully steerable, 64m diameter paraboloidal radio telescope capable to operate

with high efficiency in a wide frequency range: from 300MHz to 100GHz. Thanks to the active surface, the expected efficiency should range from the maximum value of about 63% (at  $\leq 10$ GHz) to about 35% (at  $\sim 100$ GHz). SRT will be located in the area named "Pranu Sanguni" close to the village of San Basilio, about 35km North of Cagliari, in Sardinia.

---

*Send offprint requests to:* N. D'Amico

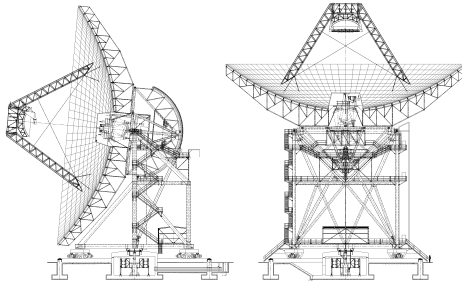


**Fig. 1.** Schematic view of SRT

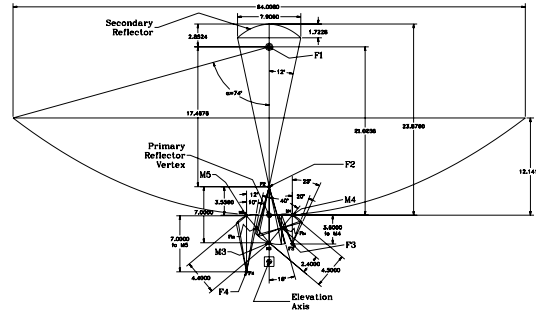


**Fig. 2.** SRT optical design

## 2. SRT design

The main antenna geometry is a shaped reflector system pair, based on the classical Gregorian configuration. A schematic view and the optical configuration are reported in Fig. 1 and Fig. 2.

Shaped primary and secondary reflector surfaces minimize the spill-over (consequently the antenna temperature) and the standing wave between secondary mirror and feeds, improving the spectroscopic performances. However the shaping adopted retains, only partially, a very desirable feature of unshaped surfaces, namely a large field of view. The primary mirror will be composed with panels supported by electro-mechanical actuators computer controlled giving the opportunity to use SRT at very high frequency.

The Gregorian configuration allows direct access to the prime focus without removing the secondary mirror; the radio telescope can switch easily receivers between the two focal positions. A rotator drum switches rapidly and automatically eight receivers at the Gregorian focus.

Additional mirrors after the Gregorian focus give the possibility to use more focal points with magnified and demagnified F/D ratio. A total of about 16 receivers may be available simultaneously on the antenna, giving the opportunity to change the operating frequency in a fast, remote and automatic way; the range of the frequencies at different focal positions are reported in Table 1.

**Table 1.** Different focal positions

Focus	$F_{min}$	$F_{max}$	F/D
$F_1$	300MHz	20GHz	0.33
$F_2$	7.5GHz	~100GHz	2.35
$F_3$	1.4GHz	35GHz	1.37
$F_4$	1.4GHz	35GHz	2.81

Prime focus receivers may reach a maximum frequency of about 20GHz, when the active surface system changes the profile of the primary mirror from shaped to parabolic geometry. Multi-feed systems can be allocated both in the primary and in the Gregorian foci. The surface accuracy of the BWG mirrors is such that a maximum frequency of 35GHz is allowed. Moreover, the F/D ratios for focal position  $F_1$  and  $F_4$  are similar to the primary and Cassegrain F/D ratios of the other two antennas operated by the INAF: Medicina and Noto; this gives us the possibility to exchange feeds and receivers between the radio telescopes.

Without controlling the surface, the radio telescope structure allows by itself operations up to about 20GHz with moderate loss of efficiency and small pointing errors. The active surface will extend the use of the instrument up to nominally 100GHz. This capability requires also a metrology system, described in Section 5, for an accurate antenna pointing.

SRT has many potentialities in different areas: radio astronomy, geodesy and space science, either as a single instrument or as part

of VLBI networks. Depending on receivers and back-end systems, SRT may span from the observation of weak sources such as pulsars or extragalactic masers to systematic surveys of galactic distributed objects both in line (molecular clouds and star forming regions) and continuum (foreground structures for Cosmic Microwave Background studies). VLBI networks will exploit the large collecting area to increase the overall sensitivity up to the millimetric ranges. When added to the existing radio telescopes in Medicina, Noto and Matera, SRT will complete a mini VLBI network whose resolution is between MERLIN and EVN.

### 3. Mechanical structure

The antenna design is based on the classical wheel-and-track configuration. The reflector consists of a backstructure which supports, through actuators, the surface composed by rings of reflecting panels. A quadrupod connected to the backstructure supports the subreflector, and the prime focus positioner and instrumentation.

The antenna is steerable about azimuth and elevation axes. The azimuth drive consists of eight torque-biased driven wheels, with the gearbox reducer spline-mounted onto the wheel shaft for maximum stiffness. The rotation about the two axes is controlled by a servo control system, and the positions are measured by 27-bit encoders. The range of motion is from  $5^\circ$  to  $90^\circ$  in elevation and  $540^\circ$  in azimuth. The servo control system consists of eight for azimuth and four for elevation identical brushless servo motors, with drivers and a position-control computer. During tracking a torque bias is applied to overcome gearbox backlash and to improve the antenna pointing accuracy.

The primary reflector surface consists of 1008 individual aluminium panels which are divided into 14 rows of principal panel types. These panels, having an area between  $2.4\text{m}^2$  and  $5.3\text{m}^2$ , are formed using aluminium sheets glued with a layer of epoxy resin at two longitudinal and several transversal slotted aluminium Z shape stiffeners. The basic back-

structure is composed by 96 radial trusses and 14 circumferential trussed hoops supported on a large center hub ring. The transfer of dish load through to the elevation bearing is accomplished by a cone-pyramid member system. The ring truss is attached at eight points to a “cone” of heavy members. The apex of this cone is coincident with a pyramid of members formed by the elevation-gear rack structure and connections to the elevation bearings. At the zenith positions, loads are transferred through this apex. The near uniform loading condition on the reflector maintains symmetry (homology) in surface deflections.

The subreflector surface consists of 49 individual aluminium panels, 48 of these are divided into 3 rows of principal panel types and one is the central panel. The panels have an average area of about  $1\text{m}^2$  and are formed using a shaped aluminium skin that is glued at two longitudinal and several transversal slotted aluminium Z shape stiffeners. The central panel is an aluminium cast design. The subreflector backstructure consists of 12 radial trusses and 3 circumferential trusses hoops supported on a center hub ring. Three of these trusses are directly connected to a triangular steel frame which has the function of a transitional structure to the six subreflector actuators. These actuators define the subreflector position, and provide for five degrees of freedom subreflector motion. These actuators are a jackscrew assembly. The drive rotation is converted to a linear motion using a backlash-free ball screw mechanism and a low backlash worm gear. The actuator drive consists of a brushless servo motor with driver. The position of the actuator is measured by incremental linear encoder.

A rotating turret (Gregorian positioner assembly) is eccentrically mounted in the focal plane of the antenna dish, and houses eight separate feed horns and associated cryogenic receiving system for operating over a range of radio frequencies from 7.5GHz to 100GHz. A drive system can rotate the turret so that any of the feed horns can be positioned in the focal plane. The system consists of a large roller bearing with internal gear and two multistage planetary gearboxes and pinions. The rotation about the axis is controlled by a servo con-

trol system, and the positions are measured by magnetic band position transducer. The range of motion is  $\pm 173^\circ$  with respect to the central position. The servo control system consists of two brushless servo motors with drivers and a position-control computer. During the rotation a torque bias is applied to overcome gearbox backlash and to improve the positioning accuracy.

A mechanism selecting among different receivers exists also in the prime focus; several boxes, depending on their dimensions, can be allocated on the side of the secondary mirror backstructure. An arm controlled by two servo motors allows, in less than four minutes, to place the required box on the prime focus. In Fig. 3 the pictures show different positions of the arm.

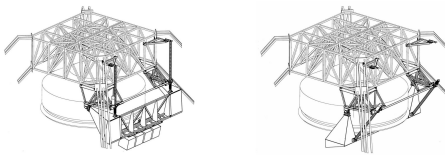


**Fig. 3.** Prime focus positioner

#### 4. Optics

Much attention has been dedicated to select the proper shaping of the Gregorian mirrors. Usually, the shaping design provides an uniform amplitude aperture field yielding an optimum gain (Rusch & Potter (1970)). In SRT mirrors design, the shaping minimizes the spill-over and the standing wave, and allows a larger focal plane than fully shaped reflectors. The energy shifts away from the blocked center region of the primary mirror, enhancing the antenna temperature efficiency and reducing the standing wave of the secondary reflector. An other benefit of this shaping design is the added taper at the main reflector edge, reducing both noise contribution and sidelobe levels.

A critical parameter of radio telescopes, especially when the mirrors are shaped, is the field of view of the antenna. A small field of

view limits the opportunity to use array of receivers in the focal plane. The performance of the antenna for off-axis scanning was intensively analyzed with respect to the classical Gregorian antenna. Electromagnetic analysis shows that feed-arrays of 5 x 5 elements may be accommodated in the Gregorian focus with a loss of 0.5dB for the extreme off-axis feed.

The surface parameter of the best-fit paraboloid of the main mirror is 21.057m focal length, while the best-fit ellipsoid of the secondary mirror has a vertex-distance of 23.172m and a foci-distance of 17.467m. The primary reflector intercept half angle at primary focus is  $74.5^\circ$  and the secondary reflector intercept half angle at Gregorian focus is  $12^\circ$ . The magnification of the Gregorian antenna is 7.15.

Two different beam-waveguide layouts are designed: BWG layout I (focus called  $F_3$ ) and BWG layout II ( $F_4$ ). The two layouts use three mirrors:  $M_3$  as shared mirror and two different mirrors  $M_4$  for the first layout and  $M_5$  for the second one. The re-imaging optics for BWG layout I was designed for maximum focal ratio reduction, from 2.35, at the Gregorian focus, to 1.37 at focus  $F_3$ ; whereas for BWG layout II it was designed such that the output focal point  $F_4$  lies beneath the elevation axis of the antenna. All the mirrors are sections of ellipsoids of revolution and present quite large aperture: 3.921 x 3.702m for  $M_3$ , 3.103 x 2.929m and 2.994 x 2.823m for  $M_4$  and  $M_5$ , respectively.

The main constraint of the reflectors is to obtain surfaces of each mirror within the design surface with RMS random surface error less than 0.3mm. The central 6cm diameter area of each mirror (i.e., around the chief-ray intersection with the surface) must be optically polished to allow the use of a laser during the alignment of the mirrors. As Fig. 4 shows, mirrors  $M_4$  (the right one) and  $M_5$  (the left one) must be mounted on the ceiling of the receiver cabin; while the support structure of mirror  $M_3$  (on the bottom of the picture) allows it to point one of the BWG layouts.

Other two different beam-waveguide layouts could be added to the actual configuration;

they will use two other mirrors with an opposite rotation of  $M_3$ .

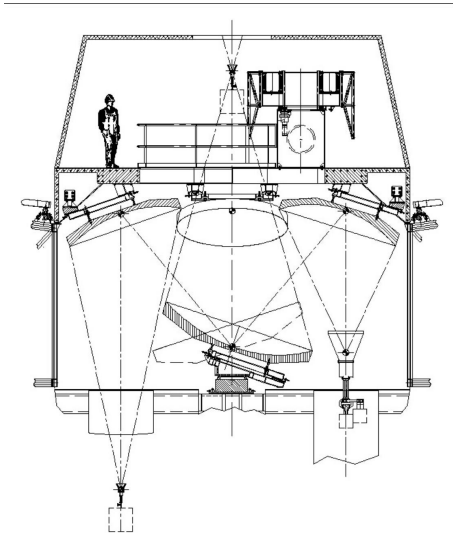


**Fig. 4.** BWG mirrors

## 5. Active Surface

In order to allow operations at high frequencies, the radio telescope will be equipped with an active surface; this concept aims to correct the gravitational effects of the antenna back-structure by moving the panels forming the primary mirror. The deformations of the surface reduce the antenna gain at the elevations other than elevation where the panels alignment is done; obviously, this effect is worst as the frequency increases.

In 2001 an active control of the primary reflector surface has been installed on the Noto 32m antenna as a prototype of the future SRT antenna. The experience on the prototype together with the results from the Finite Element analysis of the mechanical structure give an evaluation of the total surface accuracy (including panels, structure, subreflector and actuators as error source) of about  $190\mu\text{m}$  with active surface to operate up to 100GHz and about  $650\mu\text{m}$  without active surface to work

at frequencies lower than 22GHz. The active surface consists of 1116 actuators with a long stroke ( $\pm 15\text{mm}$ ) allowing to convert the primary surface from the shaped profile to the true paraboloid.

## 6. Metrology

To guarantee a good efficiency up to 100GHz, the antenna requires a state-of-art metrology to control relative and absolute position of surface and structure. The metrology will deal with the measurement of the reflector, the alignment of the subreflector and structure deformations. The target values for reflector surface control accuracy is of 0.19mm (total RMS) and the pointing precision needs an accuracy of the order of 1arcsec. In order to get these goals the experience developed in other millimeter radio telescopes, like GBT (Green Bank Telescope, USA), LMT (Large Millimeter Telescope, MEX), and IRAM (Institut de Radio Astronomie Millimétrique, E), has been also considered.

The causes of errors are divided in two main classes: repeatable errors (mechanical errors during initial alignment and gravity deformations) and, more critical, non-repeatable errors (thermal gradient and wind effects).

At this stage the metrology system is foreseen to be composed by four sub-systems. Concerning the subreflector alignment, the subsystem shall consist of a stationary laser head and a 5-D sensor able to measure five over six subreflector's degrees of freedom; the sixth degree of freedom (namely rotation around optical axis) is considered not relevant. The shift along the optical axis will be controlled by a laser ranging system, while the other 4 degrees (two shifts and two tilts) are monitored by using two Position System Devices (PSDs). The PSDs will be placed on the subreflector structure, while the laser diode will take place as close as possible to the intersection between optical axis and the main reflector. The shift accuracy and resolution (three axis) would be of the order of  $\pm 45\mu\text{m}$  and less than  $10\mu\text{m}$  respectively. The two tilts would have  $\pm 1.3\text{arcsec}$  and  $\pm 0.5\text{arcsec}$  in, respectively, accuracy and resolution. Figure 5 shows the approximate lo-

cations of the two main metrology components in relation to the rest of the telescope.

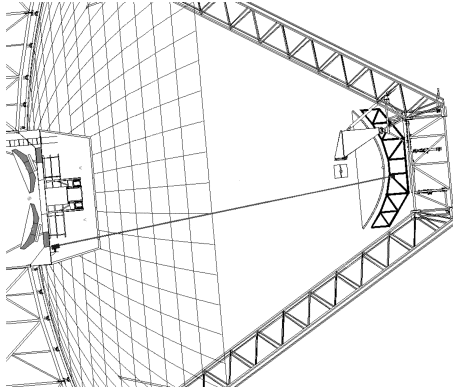


**Fig. 5.** Location of the laser metrology components

A network of temperature probes distributed on the whole structure (alidade, back-structure of the primary mirror, primary panels, quadrupod and secondary mirror) has been also foreseen; because thermal insulation and forced ventilation of the reflector backstructure, originally planned, are now postponed

this network is very crucial. The exact position of each probe will be set through a FEM analysis. The FEM software simulation, according to the values of measured temperature will drive the actuators in an open loop fashion.

The pointing model will be supported by an optical startracker.

The fourth subsystem will consist of some inclinometers that help the FEM simulation for correcting temperature deformations.

Finally, the possibility to install rangefinders on the primary reflector to control in real-time the deformations is under study. Further environmental monitoring such as wind strength or air pressure effects will be also studied.

## References

- Rusch, W.V.T., Potter, P.D., 1970, Analysis of reflector antennas, Academic Press
- Orfei, A., Morsiani, M., Zacchiroli, G., Maccaferri, G., Roda, J., 2004, "Active surface system for the new Sardinia Radiotelescope," SPIE, Astronomical Structures and Mechanisms Technology, Glasgow (UK)